Australasian Plant Pathol. (2014) 43:715–726
DOI 10.1007/s13313-014-0314-7

Proteomic analysis reveals the potential involvement of xylanase from *Pyrenophora teres* f. *teres* in net form net blotch disease of barley

I. A. Ismail · D. Godfrey · A. J. Able

Received: 25 May 2014 / Accepted: 1 September 2014 / Published online: 28 September 2014

Abstract The barley pathogen *Pyrenophora teres* f. *teres* (*Ptt*) produces proteinaceous toxins that contribute to the necrotic symptoms observed during net form net blotch (NFNB) disease. To better understand the relationship between these toxins and virulence, a proteomics approach was used to identify proteins differentially expressed in a more virulent *Ptt* isolate. Three proteins were identified: an endo-1,4-β-xylanase A (PttXyn11A), a cysteine hydrolase family protein (PttCHFP1) and an unknown (but conserved) secreted protein (PttSP1). PttXyn11A was homologous to a plant cell-wall degrading enzyme but also had a predicted necrosis-inducing region on the enzyme surface. PttCHFP1 showed homology to an isochorismatase, an enzyme proposed to suppress plant defence. Xylanase activity and *PttXyn11A* expression were greater in more virulent isolates *in vitro* and during the interaction respectively, suggesting that PttXyn11A plays a role in symptom development.

Keywords Barley net blotch · Net form net blotch · Virulence · Proteinaceous toxins · Xylanase

Introduction

Net form net blotch (NFNB), caused by the Ascomycete *Pyrenophora teres* f. *teres* (*Ptt*), is a major barley disease worldwide. The interaction between pathogenic fungi and the host plant is determined by the production of molecules from both fungus and plant (Tan et al. 2010). However, there is wide variation in the virulence on barley between *Ptt* populations (Afanasenko et al. 2007). Understanding the basis for virulence therefore is key to future disease control strategies because the evolution of virulence may determine the emergence and re-emergence of pathogens leading to host resistance being broken down and subsequent host range expansion (Sacristan and Garcia-Arenal2008).

Ptt spends most of its lifecycle acting as a necrotroph (Able 2003; Lightfoot and Able 2010). Necrotrophic fungi are well characterised as using large quantities of cell wall-degrading enzymes, such as endoxylanase, to cause diseases (Hammond-Kosack and Rudd 2008). Endoxylanase has been considered essential for the infection of various plant pathogenic fungi and has been identified in many fungal species including *Fusarium* spp. (Jaroszuk-Scisel and Kurek 2012), *Cochliobolus carbonum* (Apel et al. 1993), *Botrytis cinerea*(Brito et al. 2006) and *Sclerotinia sclerotiorum* (Ellouze et al. 2011). However, xylanase has not been previously identified in *Ptt*. Necrotrophic fungi may also produce proteinaceous toxins and/or effectors to aid colonisation of the susceptible host (Tan et al. 2010). Examples include the NIP1 effector protein secreted by the barley pathogen *Rhynchosporium commune*(Fiegen and Knogge 2002) as well as SnToxA produced by *Stagonospora nodorum* and PtrToxA and PtrToxB produced by *Pyrenophora tritici-repentis*, necessary for virulence on certain cultivars of wheat (Kwon et al. 1998; Liu et al. 2009). Previous research has identified that proteins in the culture filtrates of *Ptt* can cause NFNB symptoms in a susceptible barley cultivar (Sarpeleh et al. 2008; Ismail et al. 2014), suggesting that these filtrates may contain proteins that induce necrosis (Sarpeleh et al. 2007; Sarpeleh et al. 2008). The main objective of this research was to characterise proteins associated with symptom development and virulence by comparing protein profiles of a less virulent *Ptt* isolate with that of a more virulent isolate. For the three proteins identified as differentially expressed by the more virulent isolate, their function was predicted and their gene expression profiles

I. A. Ismail · D. Godfrey · A. J. Able (✉)
School of Agriculture, Food & Wine, The University of Adelaide, Waite Research Institute, PMB 1, Glen Osmond, SA 5064, Australia
e-mail: amanda.able@adelaide.edu.au

determined during the interaction between a susceptible barley cultivar and six isolates with different virulence.

Materials and methods

Identification of proteins associated specifically with greater virulence

The more virulent isolate, 32/98, and a less virulent isolate, 08/08f, were grown in Fries culture medium (FCM), toxin extracted and quantified as previously described (Ismail et al. 2014). The isolates were provided from the South Australian Research and Development Institute (SARDI) collection and details of their origin provided previously (Ismail et al. 2014). A two-dimensional gel electrophoresis (2DGE) proteomics approach was used to identify virulence-related proteins. Proteins were precipitated in a mixture of 0.07 % 2-mercaptoethanol(2ME) and 10 % trichloroacetic acid (TCA) in cold acetone (Méchin et al. 2007). Isoelectric focusing (IEF) was used to separate proteins based on p*I* using a Ettan IPGphor (Pharmacia Biotech Inc. Sweden) as previously described (Khoo et al. 2012). The first dimension separation was conducted using 11 cm IPG ReadyStrips pH 3-10(Bio-Rad) at 22 °C. Protein (97 μg) in solution R to a final volume of 200 μL was mixed with 0.0002 % of bromophenol blue and loaded into an Ettan IPGphor strip holder (Amersham Biosciences, UK). The strips were passively rehydrated for 30 min before separation using 50 V for 12 h (linear), 250 V for 2 h (linear), 4000 V for 4 h (linear) and 8000 V for 45000 Vhs (rapid). IPG strips were equilibrated according to Khoo et al. (2012). After equilibration, the second dimension was conducted using the Bio-Rad Criterion XT 10 % Bis-Tris IPG +1 well 11 cm 1 mm gels (BioRad) and separated according to the manufacturer's protocol. Gels were stained using a Coommassie Blue Staining protocol compatible with tandem mass spectrometry (MS/MS) (Khoo et al. 2012). Three gels representing three biological replicates for each isolate were scanned using an ImageScanner (Amersham Biosciences). The protein profiles of the more virulent and less virulent isolate were compared manually and the unique spots were then selected and sequenced at Adelaide Proteomics Centre (The University of Adelaide) using Liquid Chromatography-Electrospray Ionisation Ion-Trap Mass Spectrometry (LC-ESI-IT MS) (Thermo Fisher Scientific Inc., USA) as previously described (Aizat et al. 2013) and data was analysed using parameters previously described (Ismail et al. 2014).

Isolation of the full length of cDNA for differentially expressed proteins

Total RNA was extracted from the mycelium of the more virulent isolate (32/98) grown in FCM for 10 days using TriPure Isolation Reagent (Roche Applied Science, USA), following the manufacturer's protocol. The concentration of RNA was measured using a NanoDrop ND-100 Spectrophotometer (NanoDrop Technologies, USA) and RNA was treated with RQ1 RNase-Free DNase (Promega, USA) to remove any DNA contamination. First strand cDNA synthesis was then performed using the SuperScript III First Strand Synthesis System (Invitrogen, Life Technology, USA) with an oligo $(dT)_{12\text{-}18}$ primer. The sequences for the open reading frames for the differentially expressed proteins were then obtained by standard reverse transcriptase (RT)-PCR using the following annealing temperatures and combination of forward (F) and reverse (R) primers to amplify *PttXyn11A* (55 °C; F:5′A TGGTTGCCTTCTCTAC TATCCTC3′, R: 5′TTAAGAGCTGCTGACAGTGATGG3′); *PttCHFP1* (54 °C, F:5′ ATGAAGCTCGCTGCGCCCAT3′; R: 5′ CTAGGAGAGTGCGGGTATGAT3′); *PttSP1* (55 °C, F: 3′ATGCGCGCCTCAATCATCATC; R: 5′ CTAGCAGT AATCGCCAATGTTGTAG). The sequences of amplicons were confirmed as per the Australian Genome Research Facility Ltd (AGRF) protocol.

Bioinformatics and conserved domain analysis

Domain detection in full length cDNA clones was performed using the NCBI Conserved Domain Search Tool (http://www.ncbi.nlm.nih.gov/Structure/cdd/wrpsb.cgi, accessed November 2012); the SMART database (http://smart.embl-heidelberg.de/smart/set_mode.cgi?GENOMIC=1, accessed November 2012); the European Bioinformatics Institute (EBI), InterProScan Sequence Search (http://www.ebi.ac.uk/Tools/pfa/iprscan/, accessed November 2012) (Zdobnov and Apweiler 2001) and PROSITE (http://prosite.expasy.org/, accessed November 2012) using the default settings. Whether proteins had the N-terminal signal peptide sequence was predicted by SignalP (http:// www.cbs.dtu.dk/services/SignalP/) (Bendtsen et al. 2004). A search for potential effector domains was conducted by looking for Y/F/WxC motifs for all candidates (Godfrey et al. 2010; Morais do Amaral et al. 2012)

Multiple alignments with similar proteins were conducted using the free end gaps and MUSCLE matrix function in Geneious software (Geneious Pro 5.4.6, Biomatters Ltd, Auckland, New Zealand). Phylogenetic trees were also built based upon the Neighbour-Joining method and Jukes-Cantor method for the genetic distance model (Saitou and Nei 1987). However sequences from *P. tritici-repentis* were not used as they had 100 % similarity to each candidate from *Ptt*.

Three dimensional (3D) structure was then predicted using the I-TASSER Server (Department of Computational Medicine and Bioinformatics, University of Michigan, USA) (Roy et al. 2010) where models for other species already existed. The full length of amino acids was used to build the

3D structure for each protein by comparing multiple-threaded alignments by LOMETS and iterative TASSER assembly simulations. The 3D structure was visualised using Geneious software and only those structures with a C-score (ranged between -5 and 2) were adopted.

Gene expression during the interaction of a susceptible barley cultivar and ***Ptt*** isolates with different virulence

Barley seedlings from the susceptible cultivar Sloop were inoculated with conidia from six isolates of *Ptt* with different virulence, using the conditions previously described (Ismail et al. 2014). The isolates were provided from the South Australian Research and Development Institute (SARDI) collection and details of their origin provided previously (Ismail et al. 2014). Plants were imaged at 64, 98, 120, 144 and 168 hours post inoculation (hpi) and RNA extracted from infected leaves at seven time points (40, 64, 98, 120, 144 and 168 hpi) and cDNA synthesised, as described earlier, for use in quantitative PCR (qPCR). The qPCR analysis was carried out using *Ptt*glyceraldehyde-3-phosphate dehydrogenase (*PttGAPDH*) (EF513236) as an endogenous control. qPCR was conducted for absolute quantification of *PttXyn11A*, *PttCHFP1, PttSP1* and *PttGAPDH* using the Applied Biosystems ViiA™ 7 Real-Time PCR System and ViiA™ 7 Software (Applied Biosystems, Life Technology) and SYBR Green (iQ™ SYBR® Green supermix, Bio-Rad). Each amplification was performed in 10 μL reaction volumes containing 5 μL iQ SYBR Green Supermix, 4.6 μL of cDNA (final concentration 64 ng) and 0.4 μL primers (final concentration 4 M). The forward (F) and reverse (R) primers used were as follows: *PttXyn11A* (F:5′ATGGCTTCTTCTACTCTTTCTG GAC3′, R:5′GAGTTGACATTCTGAGCGTTCC3′), *PttCHFP1* (F:5′CGGAAATGATACCTATGACCTAACG3′, R:5′AGTCGGCTCCACTGCTTTGC3′), *PttSP1* (F:5′AATC ATCATCGCACTTTCTTCC3′, R:5′TCGTAGATGACTTC GCACTTTG3′), *PttGAPDH* (F:5′GGTCAATGGCAAGACC ATCCGCTTC3′, R:5′ACGACCTTCTTGGCTCCACCCT TC3′). C_T values and melt curves were analysed for each gene. The absolute amount of transcript was estimated in each sample using a generated linear standard curve as described by Livak and Schmittgen (2001). The absolute quantity for each gene at each time point was normalised against the *PttGAPDH* quantity at the same time point. A no-template control and a no-reverse-transcriptase control were used as negative controls while a plasmid containing the corresponding genes was used as positive control. Three biological replicates and three technical replicates were used for each time point.

Xylanase activity in isolates of ***Ptt*** with different virulence

The xylanase activity was measured in the filtrates of five *Ptt* isolates grown in FCM for 15 days at room temperature using the XYLAZYME AX kit (Megazyme, International Ireland Limited, Ireland). Proteins were extracted and quantified as described previously. Proteins were mixed with sterilised nanopure water (SNW) to a final concentration of 0.4 μg/μL in a total volume of 300 μL. Three biological replicates of each protein extract were used. Three hundred μL of SNW was added to 200 μL of control xylanase solution (*A. niger*) (approx. 275 mU/mL) as a positive control. A XYLAZYME AX tablet was placed in the sample and transferred without stirring, to a water bath at 50 °C and incubated for 30 min. Five mL of Tris Base solution (1.5 M, pH 9 with HCl) was added and stirred vigorously and incubated at room temperature for 5 min to terminate the reaction. Solutions were stirred prior to filtration using Whatman No.1 filter paper and then the absorbance measured at 590 nm. The reaction blank was prepared by the same method but using 0.5 mL SNW instead of the sample. The activity of xylanase in the filtrates of isolates from *Ptt* was calculated using the following equation:

$$\text{Xylanase activity} = \text{Added activity} \times SA/(TA-SA)$$

Where the added activity=the amount of xylanase added to the water sample (55 mU in the control xylanase solution in 200 μL), SA=sample absorbance obtained for extracts to which no control xylanase was added, TA=the total absorbance to which the control xylanase was added.

Results

Identification of proteins differentially expressed in a more virulent isolate

The 2DGE protein profiles of the culture filtrates from a less virulent isolate (08/08f) and more virulent isolate (32/98) were compared and the overall protein patterns were quite similar in both isolates (Fig. 1a and b). The majority of proteins were between 10 and 75 kDa and more abundant at 10 to 25 kDa while their isoelectric points (p*I*) were mostly in the range of 3.5 to 7.3. Two unique spots at 25 and 30 kDa were only present in the profile for the proteinaceous toxin mixtures extracted from the more virulent isolate (Fig. 1a). LC-ESI-IT MS analysis of the two spots has identified three proteins based on their peptide sequences (Table 1). Their presence in both spots is usual given the likelihood that heterogeneous phosphorylation gives a series of spots with different molecular weights and p*I* values for the same protein (Seo and Lee 2004). The identified peptides shared most similarity with a cysteine hydrolase family annotated as an isochorismatase (XP_001932705); an endo-1,4-β-xylanase A of glycosyl hydrolase family 11 (XP_001941158) and a conserved hypothetical protein (XP_001933504) from *P. tritici-repentis*, all of

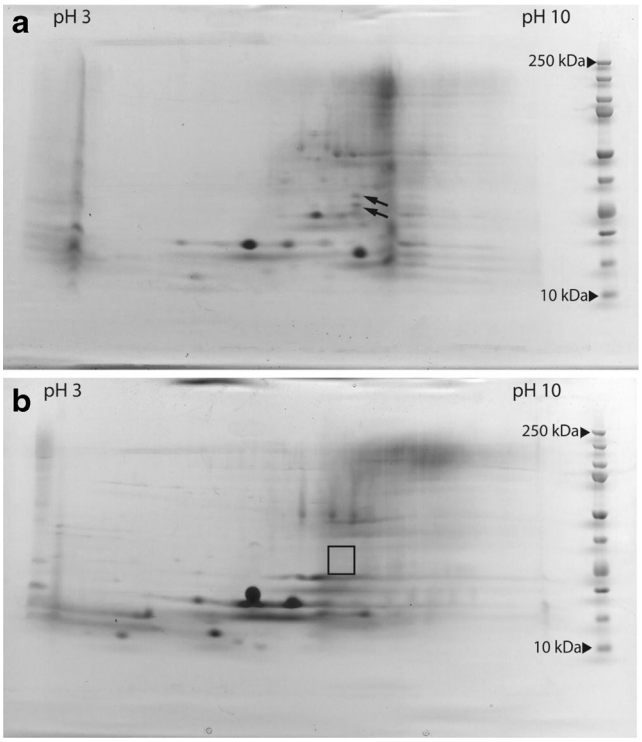

Fig. 1 Identification of proteins extracted from culture filtrates from the more virulent isolate 32/98 **a** and the less virulent isolate 08/08f **b** using 2-D gel electrophoresis. Two unique spots (black arrows) associated with the more virulent isolate were analysed using LC-ESI-IT MS (rectangled area highlights the lack of spots in the less virulent isolate) (see Table 1). Precision Plus Protein Standard was used as a marker ladder. Representative gel image for three biological replicates

which match to proteins annotated as conserved hypothetical proteins in *Ptt* (Table 1). All identified proteins from *Ptt* had an N-terminal signal peptide sequence as predicted using SignalP (Bendtsen et al. 2004), indicating that they were secreted proteins as expected.

Predicted function of the proteins differentially expressed in the more virulent isolate

The full length cDNA for each candidate was isolated and assigned a name based on function and submitted to NCBI. The candidates are referred to as *Ptt* endoxylanase 11A (PttXyn11A), *Ptt* cysteine hydrolase family protein (PttCHFP1) and *Ptt* secreted protein 1 (PttSP1) (Table 1) and have been assigned the accession numbers JX900133, JX900134 and JX900135 respectively in the NCBI database.

Sequence analysis showed that the *PttXyn11A* cDNA contained 693 bp encoding a putative protein consisting of 231 amino acids (Fig. 2a). SignalP 3.0 predicted that the N-terminal amino acid sequence has features of a signal peptide and the cleavage site was located between the 20th and 21st amino acids. The peptides identified by LC-ESI-IT MS (Table 1) matched (100 %) to residues 144 to 181 of the open reading frame for PttXyn11A (Fig. 2a). The putative protein

Table 1 Protein identification of differentially expressed two-dimensional gel electrophoresis (2DGE) protein spots (Fig. 1a) using LC-ESI-IT MS and MASCOT. The two accession numbers for each protein represent the most similarity to proteins from the *Pyrenophora teres repentis (Ptr)* and the *Pyrenophora teres* f. *teres (Ptt)* databases. The *Ptr* database was used to identify these proteins then a BLAST search identified *Ptt* proteins (as the *Ptt* database was not available at the time of identification)

Proteins identified	Accession	Identified peptides	Observed/ theoretical MW(kDa)[a]	Observed/ theoretical pI[a]	IonScore (Identity / homology threshold)[b]	Combined IonScore[b]	E value[c]	% Coverage[d]	Secreted[e]
Isochorismatase, *Ptr*	XP_001932705	1.R.NGMPVLWTFWGLDGK.D							
Hypothetical protein, *Ptt*	XP_003303790								
2.R.SALIIIDMQNFFLHPELTPSAEGGR.K25–30/ 31.15.5/7.81. 70(44/29) 2. 128(40/30)1982e^{-165}14YEndo-1,4-β-xylanase A, *Ptr* Hypothetical protein, *Ptt*XP_001941158 XP_003306630 1.K.GQVQSDGGTYDILQTTR.Y									
2.R.YNQPSIDGTQTFQQFWSVR.T25–30 /24.95.5/ 7.81. 128(43/34) 2. 105(43/-)3332e^{-129}16YConserved hypothetical protein *Ptr* Hypothetical protein *Ptt*XP_001933504 XP_003296828 1.R.TSHVYQSYNIGDYC									
2.R.QPSANLPVDSTK.L25–30 /19.95.5/ 5.91. 52(44/34) 2. 27(44/28)3555e^{-101}15Y[a] The predicted molecular weight (MW) and isoelectric point (p*I*) of the matched protein based on the values provided in the MASCOT summary report. [b] The ion scores for each of the matched peptides and the cut off score for being considered as having extensive homology are shown in the brackets. [c] Combined ion scores (the sum of individual peptide scores for the protein). [d] The percent coverage of the matched protein by the LC-ESI-IT MS derived *de novo* peptide sequences. [e] Signal peptide sequence predicted by SignalP (http:// www.cbs.dtu.dk/services/SignalP/)									

has a calculated molecular mass of 24.9 kDa. Conserved domain analysis revealed that the PttXyn11A amino acid sequence contains domains matched to the GH11 family (EC:3.2.1) (data not shown). This family contains enzymes that hydrolyse the glycosidic bond between two or more carbohydrates, were formerly known as cellulase family G (Davies and Henrissat 1995), and have xylanase (EC:3.2.1.8) activity.

Alignment of PttXyn11A, TrXyn11A and BcXyn11A of *Ptt, T. reesei,* and *B. cinerea* respectively (Brito et al. 2006; Ellouze et al. 2011) showed that *PttXyn11A* encodes two sites (LIEYYIVEDF and VAVEGYQSSGSA) which matched the conserved region (active site) of all xylanase proteins (Fig. 2b). The active sites of the protein are approximately located in the middle of the structure between residues 126 to 135 and 216 to 227. Rotblat et al. (2002) and Noda et al. (2010) also identified a necrosis-inducing region of 30 aa (aa residues 136 to 166) in the sequences of TrXyn11A and BcXyn11A of *T. reesei* and *B. cinerea* respectively. This region is similar in PttXyn11A (Fig. 2b), especially at the peptide TSDGS which has been proven to cause necrosis in tomato leaves (Noda et al. 2010). The peptides TKLGE and TEIGS in the Xyn11A sequences for *T. reesei* and *B. cinerea* respectively, have been proven to induce necrosis *in planta* for both fungi (Rotblat et al. 2002; Noda et al. 2010). However, these peptides were substituted by the peptides QKKGQ in PttXyn11A. The three dimensional structure of PttXyn11A fitted the typical xylanase profile with three helices structures and the majority of the molecule being beta sheets (Fig. 2c). The active sites and necrosis-inducing region of the protein appeared as beta sheets in the structure (Fig. 2d). PttXyn11A (Fig. 2e and f) showed great similarity to BcXyn11A, predicted by Noda et al. (2010) (Fig. 2g and h). The predicted 30 aa necrosis-inducing region, which is similar to the region in BcXyn11A (Noda et al. 2010), was located at the surface of the protein. The two necrosis sites predicted in PttXyn11A (Fig. 2e and f), displayed as beta sheets on the surface of the enzyme as they did for BcXyn11A of *B. cinerea*(Noda et al. 2010) (Fig. 2g and h).

The activity of xylanase was significantly higher ($P<0.001$, LSD=0.71) in the more virulent isolates (32/98 and 152/09) compared with the isolates with lower virulence (08/08f and 122/09) (Fig. 3).

The *PttCHFP1* cDNA contained 903 bp which encodes a putative protein consisting of 301 amino acids (Fig. 4a). A signal peptide and associated cleavage site was identified and located between amino acids 19 and 20. The peptides identified by LC-ESI-IT MS analysis (Table 1) have matched approximately to the middle of the protein at residues 57 to 110 (Fig. 4a). Conserved domain analysis suggested that PttCHFP1 belongs to the cysteine hydrolase family and that it contains the conserved *cis*-peptide bonds considered to be a conserved feature (catalytic triad) in this family. Although PttCHFP1 belongs to the cysteine hydrolase superfamily, the amino acid sequence shared similarity with a number of families in that superfamily, including isochorismatase and CSHase (N-carbamoylsarcosine amidohydrolase).

Phylogenetic analysis of selected members of cysteine hydrolase families suggested that PttCHFP1 was most likely a homolog to the isochorismatase family (Fig. 4b). BLASTp analysis also showed that PttCHFP1 matched to a *P. tritici-repentis* protein annotated as an isochorismatase and a probable isochorismatase from *Pseudomonas fluorescens* (Q51790). Although PttCHFP1 contained domains sharing homology with the isochorismatase family (spfam00857), it also shared a domain with other families (CSHase, nicotinamidase and nicotinamidase-related amidohydrolases) (data not shown).

Three dimensional modelling indicated a random similarity of PttCHFP1 (Fig. 4c) to isochorismatase and in particular, the three dimensional structure template model of the *P. aeruginosa* 1NF8 protein family (Fig. 4d) (Parsons et al. 2003).

The *PttSP1* cDNA contained 534 bp that encodes a putative protein consisting of 178 amino acids (Fig. 5a). The cleavage site for the signal peptide of the protein was located between amino acids 18 and 19. In addition, a BLASTp search identified homology to this protein, mainly from Ascomycetes, but with unknown function. PROSITE identified a prokaryotic membrane lipoprotein lipid attachment site (PS51257, PROKAR_LIPOPROTEIN) in the first 19 aa of the protein (Fig. 5a and b). This site is also found in bacterial 17kDa surface antigen proteins such as that produced by *Ricksettia* (data not shown). However, all other domain searching tools did not identify any domain in this protein. In addition, the number of cysteine residues within the mature peptide was 4.4 % while the observed percentage for cysteine in most apoplastic fungal effectors is 5 % (Morais do Amaral et al. 2012). The search for potential degenerative Y/F/WxC motifs, often identified in effectors (Godfrey et al. 2010; Morais do Amaral et al. 2012), identified the YxC motif within the first 46 amino acids of the N-terminal methionine (Fig. 5a and b). However, due to the limited information about the homologues of this protein no comparison was made with other 3D structures.

Gene expression during the interaction of a susceptible barley cultivar and *Ptt* isolates with different virulence

The virulence of the six isolates on the susceptible barley cultivar Sloop was also recorded so that it might be correlated with the expression of the candidates during the interaction. Symptom development and the timing of that development was similar to our previous work (Ismail et al 2014). Symptoms appeared after 64 hpi as small pin-point lesions in leaves infected with more virulent isolates (32/98 and 152/

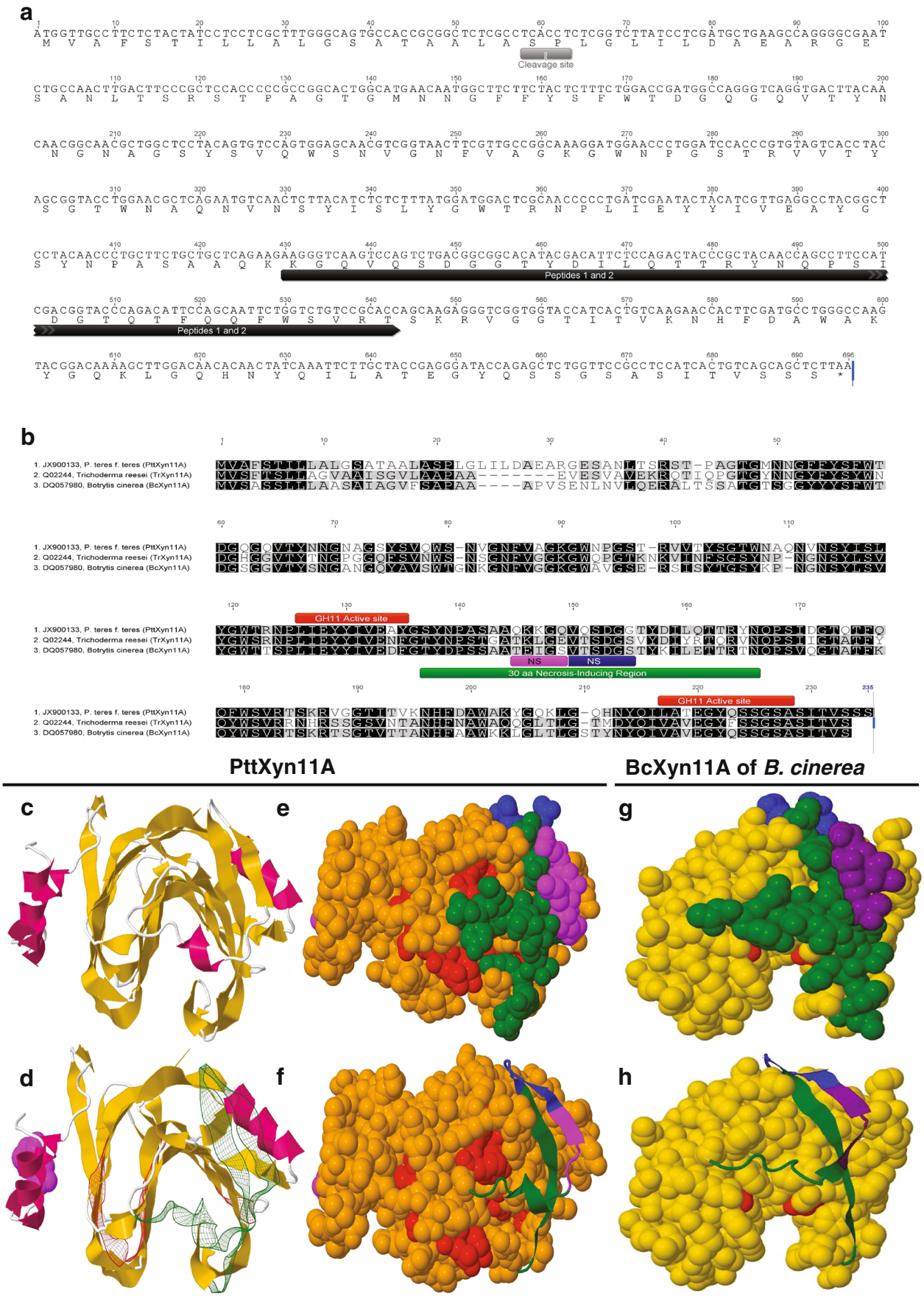
a
Cleavage site
Peptides 1 and 2
Peptides 1 and 2
b
1. JX900133, P. teres f. teres (PttXyn11A)
2. Q02244, Trichoderma reesei (TrXyn11A)
3. DQ057980, Botrytis cinerea (BcXyn11A)
GH11 Active site
NS
NS
30 aa Necrosis-Inducing Region
GH11 Active site
PttXyn11A
BcXyn11A of B. cinerea
c
d
e
f
g
h

◀ **Fig. 2** Characterisation of PttXyn11A. **a** The full length of *PttXyn11A* cDNA and PttXyn11A protein (JX900133). Cleavage site is shown in light gray bar below the sequence, identified peptides shown in black arrow below the sequence, star indicates stop codon. **b** Alignment of PttXyn11A of *Ptt* with TrXyn11A, *Trichoderma reesei* (Saarelainen et al. 1993) and BcXyn11A, *B. cinerea* (Brito et al. 2006). Selected regions of the proteins identified in the alignment are displayed: the active site (GH11) above the sequence (*red bars*), the two necrosis-inducing sites (NS) below the sequence (*purple and blue*) and the 30 aa of necrosis-inducing region identified in *B. cinerea* (Noda et al. 2010) below the sequence (*green bar*). Sequence identity shown in black bold and conserved in gray. **c** The predicted three dimensional structure of PttXyn11A of *Ptt*, the model shows the alpha helical (*deep pink*), beta strand (*orange*) and turns (*white*). **d** The active site of PttXyn11A shown in red mesh ribbon, the 30 amino acids necrosis inducing site shown in green mesh ribbon, purple balls show the cleavage site of the protein. **e** and **f** Space filling predicted 3D structure of PttXyn11A showing similarity to the template model of BcXyn11A of *B. cinerea* **g** and **h** (Noda et al. 2010), GH11 active site in red, 30 aa necrosis inducing region in green and necrosis-inducing sites in blue and purple are shown

09), but after 98 hpi in leaves infected with the less virulent isolates 08/08f, 122/09, 55/07 and 123/09 (Fig. 6d). By 98 hpi, necrotic lesions were well developed in leaves infected by 32/98 or 152/09. The appearance of necrosis in the leaves infected with 08/08f, 122/09 and 123/09 was delayed until 144 hpi and 120 hpi in 55/07.

All *Ptt* isolates expressed the three genes during the plant-pathogen interaction (Fig. 6a, b and c). However, in general, the absolute normalised quantity of *PttXyn11A* was much higher than that for the other two genes (Fig. 6a). *PttXyn11A* transcript production by the six isolates *in planta* during the interaction was similar until 98 hpi such that by 168 hpi the most virulent isolates (32/98 and 152/09) produced significantly more *PttXyn11A* ($P<0.001$, LSD=6.08) compared with less virulent isolates (Fig. 6a). There were no significant differences in expression of *PttCHFP1* and *PttSP1* for the six isolates across time (Fig. 6b and c).

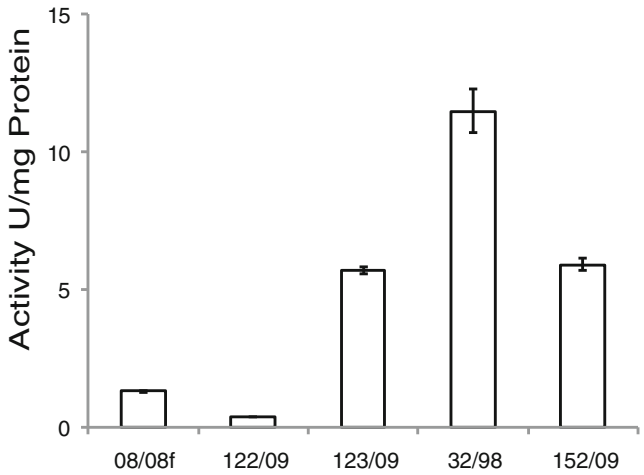

Fig. 3 Activity of xylanase in the culture filtrate of six isolates of *Ptt* grown in FCM for 15 days. Isolates listed from left to right in order of virulence (Ismail et al 2014). Three biological replicates, the least significant difference (LSD)=1.171 at $P<0.001$. Error bars represent the standard error of three biological replicates

Discussion

Three proteins were detected in the culture filtrates of the more virulent isolate 32/98 (PttXyn11A, PttCHFP1 and PttSP1) but not for the less virulent isolate 08/08f. The full length of the cDNA for the three candidates were successfully isolated using RT-PCR and bioinformatics analysis confirmed that they were probably encoding an endo-1,4-ß-xylanase (PttXyn11A), a cysteine hydrolase family protein (PttCHFP1) and a secreted protein with unknown function (PttSP1) respectively. These proteins were also confirmed across a number of isolates with varying virulence. The observation that the more virulent isolates had significantly greater xylanase activity *in vitro* (Fig. 3) and *PttXyn11A* expression *in planta* (Fig. 6a) compared with less virulent isolates also suggests a role for PttXyn11A in disease development. Regardless of the virulence of the isolate, transcripts of *PttXyn11A*, *PttCHFP1* and *PttSP1* were detected *in planta* suggesting the potential role of proteinaceous toxins in fungal growth and therefore the infection process of *Ptt*. In particular, transcripts of *PttXyn11A* were abundantly expressed by the more virulent isolates (32/98 and 152/09) *in planta*.

The function of each candidate was predicted by identifying the conserved region in the open reading frame from the cDNA isolated from *Ptt*. Phylogenetic and conserved domain analysis revealed that PttXyn11A shares similarity to the GH11 family and has strong homology to the well characterised TrXyn11A and BcXyn11A (Brito et al. 2006; Noda et al. 2010; Ellouze et al. 2011). Moreover, PttXyn11A showed all the characteristics of the GH11 endo-β-1,4-xylanases, including the basic p*I* and low molecular weight that are common for this group; the typical jelly-roll topology structure of the GH11 family with two twisted β-sheets enclosing a substrate-binding cleft (Hakulinen et al. 2003); and a 30 aa necrosis-inducing region (Saarelainen et al. 1993; Noda et al. 2010). Xylanase plays an important role in virulence in many fungal species (Gomez-Gomez et al. 2001; Brito et al. 2006; Noda et al. 2010; Jaroszuk-Scisel and Kurek 2012) through degradation of the plant cell wall components such as xylans (Beliën et al. 2006; Jaroszuk-Scisel and Kurek 2012) providing access to the cell and converting complex plant material into readily assimilated nutrients for the fungus to grow faster (Noda et al. 2010). *PttXyn11A* gene expression was upregulated in the more virulent isolates (especially by 168 hpi when symptoms are most obvious) suggesting that xylanase may act as a virulence factor as has been observed for *B. cinerea* (Brito et al. 2006; Noda et al. 2010). Mutation of this enzyme in *B. cinerea* resulted in reduction of

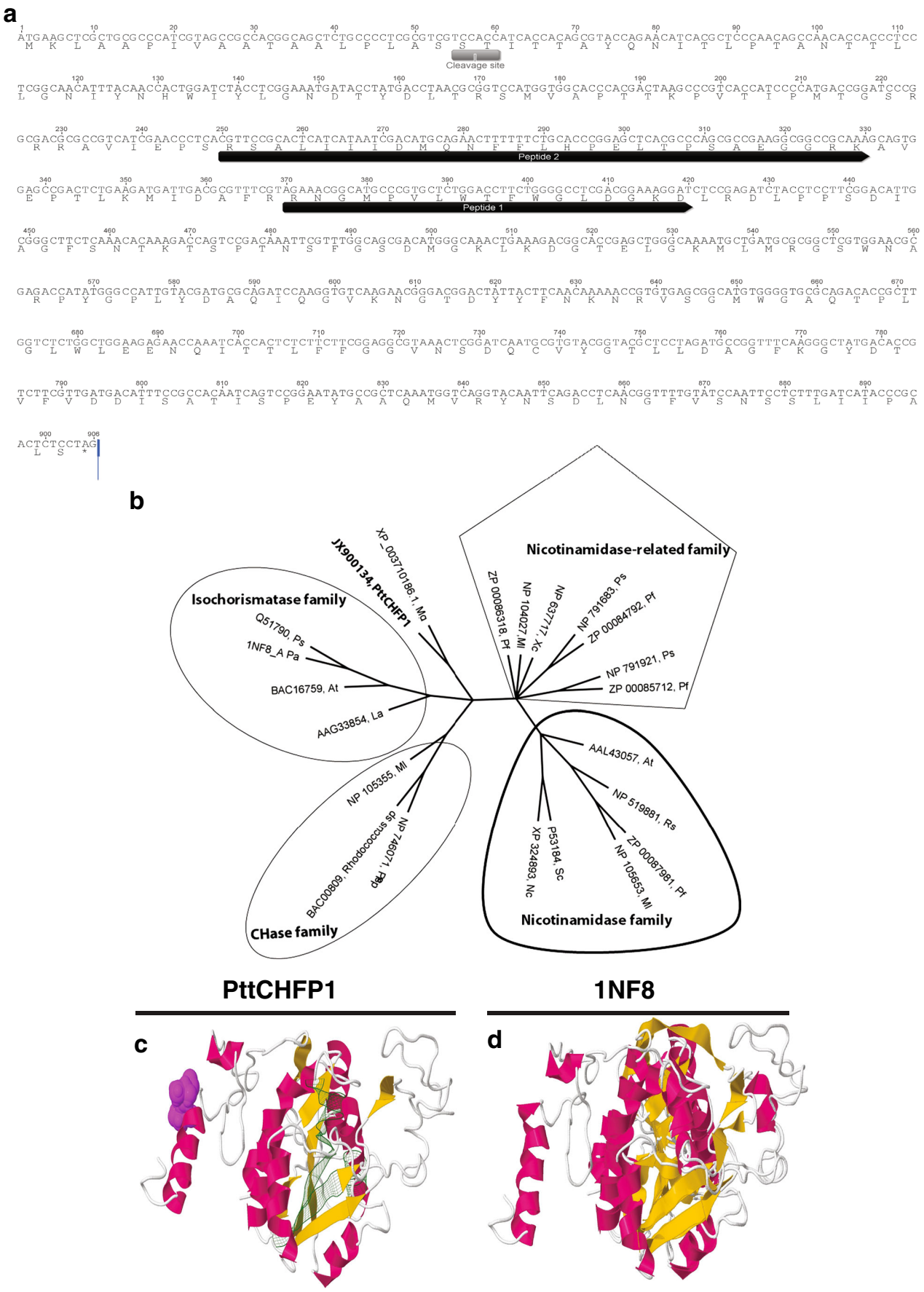
a
Cleavage site
Peptide 2
Peptide 1
b
Nicotinamidase-related family
Isochorismatase family
CHase family
Nicotinamidase family
JX900134, PttCHFP1
XP_003710186.1, Mg
Q51790, Ps
1NF8_A Pa
BAC16759, At
AAG33854, La
ZP 00086318, Pf
NP 104027, Ml
NP 637717, Xc
NP 791683, Ps
ZP 00084792, Pf
NP 791921, Ps
ZP 00085712, Pf
NP 105355, Ml
BAC00809, Rhodococcus sp
NP 746071, Pap
AAL43057, At
NP 519881, Rs
XP 324893, Nc
P53184, Sc
ZP 00087981, Pf
NP 105653, Ml
PttCHFP1
1NF8
c
d

◀ **Fig. 4** The full length of *PttCHFP1* cDNA and PttCHFP1 protein (JX900134) **a**. Cleavage site is shown in light gray bar below the sequence, identified peptides shown in dark gray arrows below the sequence, asterisk below the sequence indicates stop codon. **b** Phylogenetic tree of selected members of the cysteine hydrolase superfamily. La; *Listonella anguillarum,* At*; Agrobacterium tumefaciens,* Pf*; Pseudomonas fluorescens,* Pa*; Pseudomonas aeruginosa,* Mo*; Magnaporthe grisea,* Ml*; Mesorhizobium loti,* Pp*; Pseudomonas putida,* Sc*; Saccharomyces cerevisiae,* Nc*; Neurospora crassa,* Rs*; Ralstonia solanacearum,* Ps*; Pseudomonas syringae,* Xc*; Xanthomonas campestris*. **c** The predicted three dimensional structure of PttCHFP1 of *Ptt*. The model shows the alpha helical (*deep pink*), beta strand (*orange*) and turns (*white*) secondary structure, multiple domains of PttCHFP1 shown in green mesh, purple balls indicate the cleavage site. **d** The 3D structure of 1NF8 template model, an isochorismatase from *P. aeruginosa* (Parsons et al. 2003)

secondary lesions on tomato leaves (Brito et al. 2006) while mutation of xylanase genes in *Magnaporthe oryzae* resulted in a reduction of the number of lesions, rate of penetration and extent of infected rice cells (Nguyen et al. 2011), suggesting that xylanases play a role *in planta* in vertical penetration and horizontal expansion by fungi. The necrosis-inducing region in BcXyn11A of *B. cinerea* and TrXyn11A of *T. reesei* showed similarity in the primary and tertiary structure to PttXyn11A (Fig. 2b,g and h) (Brito et al. 2006; Noda et al. 2010). In addition, this region was located at the surface of the enzyme confirming similarity to the well characterised BcXyn11A of *B. cinerea* (Noda et al. 2010). This region may contribute directly to necrosis via the necrosis-inducing region of the

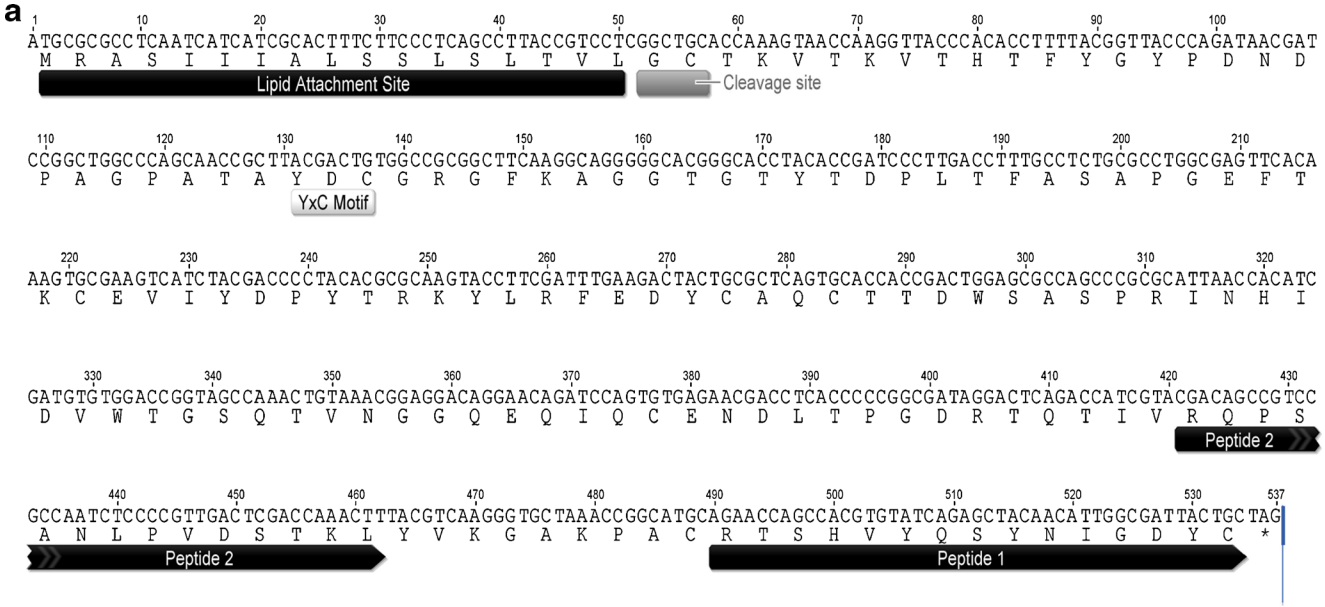

Fig. 5 The full length of PttSP1 cDNA and PttSP1 protein **a**. Lipid attachment site is shown in black bar below the sequence. Cleavage site is shown in light gray bar below the sequence, identified peptides shown in dark gray arrows below the sequence, YxC motif is also shown while star indicates stop codon. **b** The predicted three dimensional structure of PttSP1 of Ptt. The model shows the alpha helical structure (*deep pink*), beta strand (*orange*) and turns (*white*) secondary structure. The predicted cleavage site is shown as purple ball, lipid attachment site is shown in red mesh and YxC motif shown in green mesh

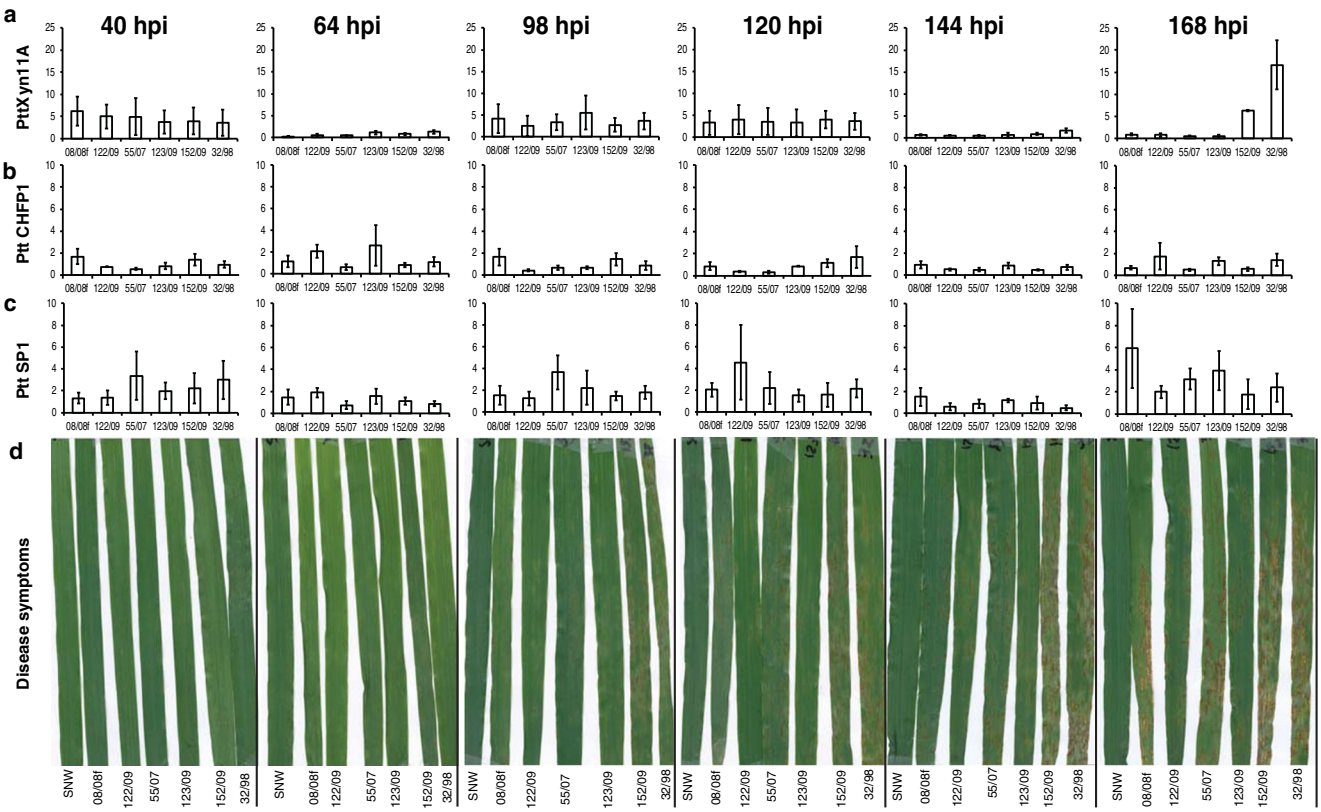

Fig. 6 The transcript expression of of *PttXyn11A* **a**, *PttCHFP1* **b** and *PttSP1* **c** during the interaction of *Ptt* isolates and a susceptible barley cultivar. The absolute amount of gene transcript was measured using qPCR and normalised relative to *PttGAPDH* in three technical replicates of three biological replicates. **d** Representative images of symptoms caused by *Ptt* isolates on barley cultivar Sloop at each timepoint is also shown for three biological replicates. SNW; sterile nanopure water was used as a control. The least significant difference (LSD) at $P<0.01$ for gene expression of *PttXyn11A*=6.5

protein, and is considered to be independent of its catalytic activity as a xylanase (Noda et al. 2010). This necrosis-inducing function has been proven in *Trichoderma viride* (Furman-Matarasso et al. 1999), *B. cinerea*(Noda et al. 2010) and *T. reesei* (Enkerli et al. 1999). The observation that *PttXyn11A* is expressed more in the more virulent isolates (where necrosis is greater) supports a similar function in *Ptt*. PttXyn11A could also act by killing the plant tissue surrounding the infected area allowing *Ptt* to grow on dead tissue. Necrotrophic fungi often promote programmed cell death by signaling to the hosts to kill themself, as a defence mechanism, prior to their invasion (Noda et al. 2010). A similar mechanism has been proposed for *P. teres* on susceptible barley (Able 2003). A role for PttXyn11A in virulence by degrading the cell wall or inducing necrosis directly (or both) remains to be confirmed through mutant analysis of *PttXyn11A*. However, a reliable transformation system has not been established for Australian isolates yet. Although there have been attempts to knock out some genes in *Ptt*, results to date have not been successful (Simon Ellwood, personal communication).

PttCHFP1 belongs to the cysteine hydrolase super family and appeared to most likely belong to the isochorismatase family by having homology to many domains (Fig. 4b). In addition, PttCHFP1 showed homology to another member of the cysteine hydrolase super family, CSHase which is involved in creatine metabolism and nicotinamidase, converting nicotinamide to nicotinic acid and ammonia in the pyridine nucleotide cycle. Gardiner et al. (2012) recently reported that cereal pathogens produce amidohydrolase proteins that might have a role in pathogenicity towards plants. These proteins are believed to have been horizontally transferred from bacteria (Gardiner et al. 2012). Bioinformatic analysis showed that PttCHFP1 also has shared homology with bacterial amidohydrolase proteins, supporting the Gardiner et al. (2012) findings. Isochorismatase has been shown to inhibit salicylic acid (SA) production through the removal of the precursor isochorismate to repress plant defences against biotrophic pathogens (Wildermuth et al. 2001; Soanes et al. 2008; El-Bebany et al. 2010). However, resistance against necrotrophic pathogens is thought to involve the jasmonic acid (JA)-signaling pathway which antagonises SA signaling and vice versa (Rahman et al. 2012). El Oirdi et al. (2011) and Rahman et al. (2012) found that *B. cinerea* manipulates the antagonistic effect between SA and JA to promote

its disease development in tomato. Thus, PttCHFP1 may allow a similar strategy for *Ptt*, especially given the constitutive expression of *PttCHFP1* for all isolates *in planta*.

PttSP1 showed similarity to other proteins with a membrane lipoprotein lipid attachment site. This site includes attachment of glyceride-fatty acid lipids which have been proposed to anchor proteins in the membrane as a part of membrane lipoprotein synthesis (Hayashi and Wu 1990). In addition, PttSP1 showed homology to a 17 kDa surface antigen protein from bacterial species. Ellwood et al. (2010) predicted several secreted surface antigens using both WolfPSORT and SignalP in the *Ptt* genome and these proteins were annotated as pathogenesis proteins. The YxC motif was identified at 44 to 46 aa (Fig. 5) and in general, if this motif is located in the first 45 amino acids of the secreted protein, this protein is considered as a candidate secreted effector protein (Godfrey et al. 2010; Morais do Amaral et al. 2012). qPCR at seven time points did not show differences in the level of *PttSP1* between isolates *in planta*. Although the expression of *PttCHFP1* and *PttSP1* were not significantly different between all isolates, sufficient protein may have been translated to be effective in the pathogenesis process. Previous research found that only trace amounts of Ptr-ToxB from *P. tritici repentis*(Kim and Strelkov 2007) and proteinaceous toxins from *Ptt*(Sarpeleh et al. 2007) were required to induce symptoms in wheat and barley respectively.

Identification and characterisation of these virulence candidate proteins (PttXyn11A, PttCHFP1 and PttSP1) from *Ptt* has provided a better understanding of how *Ptt* may infect barley and might ultimately help to develop appropriate disease control strategies. *Ptt* isolates, especially more virulent isolates, produce PttXyn11A in a greater quantity to either degrade the plant cell wall providing entry to the host cell and the nutrients necessary for fungal development, or by inducing programmed cell death. In addition, if PttCHFP1 is an isochorismatase then the plant defence response might be suppressed (Soanes et al. 2008) and the fungus would be able to grow rapidly in the plant. The contribution of individual proteins to net blotch disease development in barley will be the focus of future research.

Acknowledgments We thank Dr Hugh Wallwork, South Australian Research and Development Institute (SARDI), for providing *Ptt* isolates and the Grains Research and Development Corporation (GRDC) for supporting this research. IAI was supported by a scholarship from the Iraqi Ministry of Higher Education and Scientific Research.

References

Able AJ (2003) Role of reactive oxygen species in the response of barley to necrotrophic pathogens. Protoplasma 221:137–143

Afanasenko OS, Mironenko NV, Filatova OA, Serenius M (2007) Structure of *Pyrenophora teres* f. *teres* populations from Leningrad Region and Finland by virulence. Mikol Fitopatol 41:261–268

Aizat WM, Able JA, Stangoulis JCR, Able AJ (2013) Proteomic analysis during capsicum ripening reveals differential expression of ACC oxidase isoform 4 and other candidates. Funct Plant Biol 40:1115–1128

Apel PC, Panaccione DG, Holden FR, Walton JD (1993) Cloning and targeted gene disruption of *xyl1*, a beta-1,4-xylanase gene from the maize pathogen *Cochliobolus carbonum*. Mol Plant-Microbe Interact 6:467–473

Beliën T, Van Campenhout S, Robben J, Volckaert G (2006) Microbial endoxylanases: Effective weapons to breach the plant cell-wall barrier or, rather, triggers of plant defense systems? Mol Plant-Microbe Interact 19:1072–1081

Bendtsen JD, Jensen LJ, Blom N, von Heijne G, Brunak S (2004)Feature-based prediction of non-classical and leaderless protein secretion. Protein Eng Des Sel 17:349–356

Brito N, Espino JJ, Gonzalez C (2006) The endo-beta-1,4-xylanase Xyn11A is required for virulence in *Botrytis cinerea*. Mol Plant-Microbe Interact 19:25–32

Davies G, Henrissat B (1995) Structures and mechanisms of glycosyl hydrolases. Structure 3:853–859

El-Bebany AF, Rampitsch C, Daayf F (2010) Proteomic analysis of the phytopathogenic soilborne fungus *Verticillium dahliae* reveals differential protein expression in isolates that differ in aggressiveness. Proteomics 10:289–303

El Oirdi M, Abd El Rahman T, Rigano L, El Hadrami A, Rodriguez MC, Daayf F, Vojnov A, Bouarab K (2011)*Botrytis cinerea* manipulates the antagonistic effects between immune pathways to promote disease development in tomato. Plant Cell 23:2405–2421

Ellouze OE, Loukil S, Marzouki MN (2011) Cloning and molecular characterization of a new fungal xylanase gene from *Sclerotinia sclerotiorum* S2. BMB Rep 44:653–658

Ellwood SR, Liu ZH, Syme RA, Lai ZB, Hane JK, Keiper F, Moffat CS, Oliver RP, Friesen TL (2010) A first genome assembly of the barley fungal pathogen *Pyrenophora teres f. teres*. Genome Biol 11:1–14

Enkerli J, Felix G, Boller T (1999) The enzymatic activity of fungal xylanase is not necessary for its elicitor activity. Plant Physiol 121: 391–397

Fiegen M, Knogge W (2002) Amino acid alterations in isoforms of the effector protein NIP1 from *Rhynchosporium secalis* have similar effects on its avirulence- and virulence-associated activities on barley. Physiol Mol Plant Pathol 61:299–302

Furman-Matarasso N, Cohen E, Du Q, Chejanovsky N, Hanania U, Avni A (1999) A point mutation in the ethylene-inducing xylanase elicitor inhibits the β-1-4-endoxylanase activity but not the elicitation activity. Plant Physiol 121:345–352

Gardiner DM, McDonald MC, Covarelli L, Solomon PS, Rusu AG, Marshall M, Kazan K, Chakraborty S, McDonald BA, Manners JM (2012) Comparative pathogenomics reveals horizontally acquired novel virulence genes in fungi infecting cereal hosts. PLoS Pathog 8:1–22

Godfrey D, Bohlenius H, Pedersen C, Zhang ZG, Emmersen J, Thordal-Christensen H (2010) Powdery mildew fungal effector candidates share N-terminal Y/F/WxC-motif. BMC Genomics 11:1–13

Gomez-Gomez E, Roncero MIG, Di Pietro A, Hera C (2001) Molecular characterization of a novel endo-beta-1,4-xylanase gene from the vascular wilt fungus *Fusarium oxysporum*. Curr Genet 40:268–275

Hakulinen N, Turunen O, Janis J, Leisola M, Rouvinen J (2003)Three-dimensional structures of thermophilic beta-1,4-xylanases from *Chaetomium thermophilum* and *Nonomuraea flexuosa*-Comparison of twelve xylanases in relation to their thermal stability. Eur J Biochem 270:1399–1412

Hammond-Kosack KE, Rudd JJ (2008) Plant resistance signalling hijacked by a necrotrophic fungal pathogen. Plant Signal Behav 3: 993–995

Hayashi S, Wu HC (1990) Lipoproteins in bacteria. J Bioenerg Biomembr 22:451–471

Ismail IA, Godfrey D, Able AJ (2014) Fungal growth, proteinaceous toxins and virulence of *Pyrenophora teres f. teres* on barley. Australas Plant Pathol doi: 10.1007/s13313-014-0295-6.

Jaroszuk-Scisel J, Kurek E (2012) Hydrolysis of fungal and plant cell walls by enzymatic complexes from cultures of *Fusarium* isolates with different aggressiveness to rye (*Secale cereale*). Arch Microbiol 194:653–665

Khoo KH, Able AJ, Chataway TK, Able JA (2012) Preliminary characterisation of two early meiotic wheat proteins after identification through 2DGE proteomics. Funct Plant Biol 39:222–235

Kim YM, Strelkov SE (2007) Heterologous expression and activity of Ptr ToxB from virulent and avirulent isolates of *Pyrenophora tritici repentis*. Can J Plant Pathol 29:232–242

Kwon CY, Rasmussen JB, Meinhardt SW (1998) Activity of Ptr ToxA from *Pyrenophora tritici repentis* requires host metabolism. Physiol Mol Plant Pathol 52:201–212

Lightfoot DJ, Able AJ (2010) Growth of *Pyrenophora teres in planta* during barley net blotch disease. Australas Plant Pathol 39:499–507

Liu Z, Faris JD, Oliver RP, Tan K-C, Solomon PS, McDonald MC, McDonald BA, Nunez A, Lu S, Rasmussen JB, Friesen TL (2009) SnTox3 acts in effector triggered susceptibility to induce disease on wheat carrying the Snn3 gene. PLoS Pathog 5:e1000581

Livak KJ, Schmittgen TD (2001) Analysis of relative gene expression data using real-time quantitative PCR and the 2(T)(-Delta Delta C) method. Methods 25:402–408

Méchin V, Damerval C, Zivy M (2007) Total protein extraction with TCA-Acetone. In 'Plant Proteomics: Methods and Protocols. Vol. 335.' (Eds H Thiellement, V Méchin, C Damerval and M Zivy) pp. 1-8. (Humana Press Inc: Totowa, NJ, USA)

Morais Do Amaral A, Antoniw J, Rudd JJ, Hammond-Kosack KE (2012) Defining the predicted protein secretome of the fungal wheat leaf pathogen *Mycosphaerella graminicola*. PLoS One 7:e49904

Nguyen QB, Itoh K, Van Vu B, Tosa Y, Nakayashiki H (2011) Simultaneous silencing of endo-β-1,4 xylanase genes reveals their roles in the virulence of *Magnaporthe oryzae*. Mol Microbiol 81:1008–1019

Noda J, Brito N, Gonzalez C (2010) The *Botrytis cinerea* xylanase Xyn11A contributes to virulence with its necrotizing activity, not with its catalytic activity. BMC Plant Biol 10:1–15

Parsons JF, Calabrese K, Eisenstein E, Ladner JE (2003) Structure and mechanism of *Pseudomonas aeruginosa* PhzD, an isochorismatase from the phenazine biosynthetic pathway. Biochemistry 42:5684–5693

Rahman TAE, Oirdi ME, Gonzalez-Lamothe R, Bouarab K (2012) Necrotrophic Pathogens Use the Salicylic Acid Signaling Pathway to Promote Disease Development in Tomato. Mol Plant-Microbe Interact 25:1584–1593

Rotblat B, Enshell-Seijffers D, Gershoni JM, Schuster S, Avni A (2002) Identification of an essential component of the elicitation active site of the EIX protein elicitor. Plant J 32:1049–1055

Roy A, Kucukural A, Zhang Y (2010) I-TASSER: a unified platform for automated protein structure and function prediction. Nat Protoc 5: 725–738

Saarelainen R, Paloheimo M, Fagerström R, Suominen P, Nevalainen KMH (1993) Cloning, sequencing and enhanced expression of the *Trichoderma reesei* endoxylanase II (pI 9) gene *xln2*. Molec Gen Genet 241:497–503

Sacristan S, Garcia-Arenal F (2008) The evolution of virulence and pathogenicity in plant pathogen populations. Mol Plant Pathol 9: 369–384

Saitou N, Nei M (1987) The neighbor-joining method - a new method for reconstructing phylogenetic trees. Mol Biol Evol 4:406–425

Sarpeleh A, Wallwork H, Catcheside DEA, Tate ME, Able AJ (2007) Proteinaceous metabolites from *Pyrenophora teres* contribute to symptom development of barley net blotch. Phytopathology 97: 907–915

Sarpeleh A, Wallwork H, Tate ME, Catcheside DEA, Able AJ (2008) Initial characterisation of phytotoxic proteins isolated from *Pyrenophora teres*. Physiol Mol Plant Pathol 72:73–79

Seo J, Lee KJ (2004)Post-translational modifications and their biological functions: Proteomic analysis and systematic approaches. J Biochem Mol Biol 37:35–44

Soanes DM, Alam I, Cornell M, Wong HM, Hedeler C, Paton NW, Rattray M, Hubbard SJ, Oliver SG, Talbot NJ (2008) Comparative genome analysis of filamentous fungi reveals gene family expansions associated with fungal pathogenesis. PLOS One 3:e2300

Tan K, Oliver RP, Solomon PS, Moffat CS (2010) Proteinaceous necrotrophic effectors in fungal virulence. Funct Plant Biol 37: 907–912

Wildermuth MC, Dewdney J, Wu G, Ausubel FM (2001) Isochorismate synthase is required to synthesize salicylic acid for plant defence. Nature 414:562–565

Zdobnov EM, Apweiler R (2001) InterProScan – an integration platform for the signature-recognition methods in InterPro. Bioinformatics 17:847–848